Transmutation Effects in Nuclear Reactors

R. Lott

March 1973

UWFDM-63

FUSION TECHNOLOGY INSTITUTE

UNIVERSITY OF WISCONSIN

MADISON WISCONSIN

Transmutation Effects in Nuclear Reactors

R. Lott

Fusion Technology Institute
University of Wisconsin
1500 Engineering Drive
Madison, WI 53706

http://fti.neep.wisc.edu

March 1973

UWFDM-63

TRANSMUTATION EFFECTS IN NUCLEAR REACTORS

Randy Lott

March 1973

FDM 63

University of Wisconsin

Introduction

Transmutations take place in all nuclear reactors. Radioactivity is induced in the structural materials of all reactors through the transmutation of stable nuclei. In fission reactors, a small amount of structural material is involved and the major source of radioactivity is the spent fuel. However, in a fusion reactor, large[12-15] amounts of structural material will be subjected to high neutron fluxes and the radioactivity associated with this material becomes important. In fast reactors,[18-21] gas production through (n,α) and (n,p) reactions can cause severe embrittlement of stainless steel. Hydrogen and helium may also expedite the nucleation of voids in the material.

Gas production in the first wall of a fusion reactor[16,17] may be more of a problem than gas production in fast reactors. In the lifetime of a fusion reactor, the composition of the structural material may be changed significantly by transmutations. This could also be a serious problem if the mechanical properties of the material are affected. Once a fusion reactor is built and operated, replacement or repair of the first wall will be a major undertaking.

This paper will present some original calculations for transmutation rates in fusion reactors. All of these calculations are based on the University of Wisconsin design of a Tokamak type reactor, as it was presented at the Austin, Texas Meeting.[1] This reactor, which will be referred to as the UWCTR, operates at a relatively low wall

loading of .53 MW/m^2. However, the results of these calculations have been normalized to 1 MW/m^2 and may be extended to other reactors.

Reaction Rates

The specific reaction rate (reactions/ $sec \cdot cm^3$) for any neutron-nuclear interaction depends on three quantities. The first quantity is the number density of target nuclei, N, which varies only slightly with irradiation conditions and is relatively easy to determine. The second and third quantities, the neutron flux and the reaction cross section are functions of energy and complicate any calculations of the reaction rate. To calculate a reaction rate, detailed knowledge of the energy dependence of the flux and cross section is required.

Because the neutron energy spectrum may range from millions of electron volts down to a small fraction of an electron volt, energies are usually expressed in terms of lethargy, u, where

$$u = \ln \frac{E\ max}{E}$$

Then a lethargy dependent flux $\phi(u)$ can be defined as the number of neutrons with lethargy u passing through a unit area per second. Also, a lethargy dependent cross section $\sigma(u)$ can be defined as the cross section for interactions with neutrons having lethargy, u. For an arbitrary neutron energy spectrum, the total reaction rate, R, is:

$$R = N \int_0^\infty \sigma(u)\phi(u)du$$

The neutron energy spectrum is then divided into groups of equal lethargy units. The number of groups, n, that is used depends on the calculation to be made. Two new quantities can now be defined

for each lethargy group, the group flux ϕg and the group cross section, σg

$$\phi_g = \int_{u_{(g-1)}}^{u_g} \phi(u)du$$

$$\sigma_g = \frac{1}{\phi g} \int_{u_{(g-1)}}^{u_g} \sigma(u)\ \phi(u)du$$

Notice that the total reaction rate can now be written, without loss of generality as:

$$R = N \sum_{g=1}^{n} \phi g\ \sigma g$$

In calculating the group cross section, it is often necessary to make some simplifying assumptions. If enough energy groups have been used to make the flux fairly constant over any specific interval, it might be assumed that

$$\phi(u) = \text{constant in interval } g = A$$

$$\phi g = A[u_g - u_{g-1}] = A\Delta u$$

$$\sigma_g = \frac{\int_{u(g-1)}^{u_g} \sigma(u)du}{\Delta u}$$

This form of the group cross section is relatively easy to evaluate numerically, if tables of cross sections are available. Other weighting functions, such as a 1/E spectrum for thermal reactors, can be used to calculate group cross sections. These cross sections must then be folded into predicted or measured values of the group flux.

Neither the flux nor the cross section can be measured directly, both must be inferred from the reaction rate. By measuring the total

number of reaction products, I, produced in some time t, the reaction rate can be calculated. If the reaction product is not produced in copious amounts and is not radioactive, measurements of the amount produced may be very difficult and unreliable. If either the flux spectrum or the cross section is well-known, the opposite quantity may be inferred from the relation

$$I = Rt = Nt \int_0^\infty \sigma(u)\phi(u)du$$

Most measurements of $\sigma(u)$ are made with mono-energetic sources of neutrons, so $\phi(u)$ can be approximated by a δ function and the integral easily solved. Spectral averaged cross sections, $\bar{\sigma}$, are also reported, where

$$\bar{\sigma} = \frac{I}{Nt \int_0^\infty \phi(u)du} = \frac{I}{N\Phi t}$$

The inclusion of the total fluence, Φt, makes this type of cross section only meaningful for a particular flux spectrum. Measurements of this type are made in EBR-II and applied to the design of other fast reactors. To measure flux spectra, materials with well known cross sections must be irradiated and the flux deduced from the relative amounts of different reaction products found in the materials.

Flux Spectrum

The types of transmutations that take place in any reactor are determined by the flux spectrum. The flux spectrum is very sensitive to position in the reactor as well as the type of reactor being considered. The flux in the cladding of a fuel pin for a thermal reactor is very different from the flux in any other structural component, even though both materials being considered may be the same. In a fast reactor, where there is very little moderation of the neutrons, the changes of flux spectrum with position are not so drastic within the core. In a fusion reactor, the shape of the flux varies with position in the blanket as neutrons are being produced, absorbed and moderated in all parts of the blanket. The flux spectrum is constantly changing with time, as the nuclear properties of the material in the reactor are changing with burn up. In fission reactors, where revisions of core geometry are relatively simple, the flux spectrum may also change with the fuel cycle. Although the flux spectrum varies between individual reactors, it is reasonable to divide nuclear reactors into three major classes - thermal, fast breeder, and fusion - and consider a general flux spectrum for each class. In Figure Ia, the flux spectrum is compared to the calculated flux spectrum for the first wall of the UWCTR. Even though the fusion reactor operates at a much higher power level, the flux levels in all groups below seven MeV are small when compared to the fission reactors. However, the large number of neutrons with high energies,

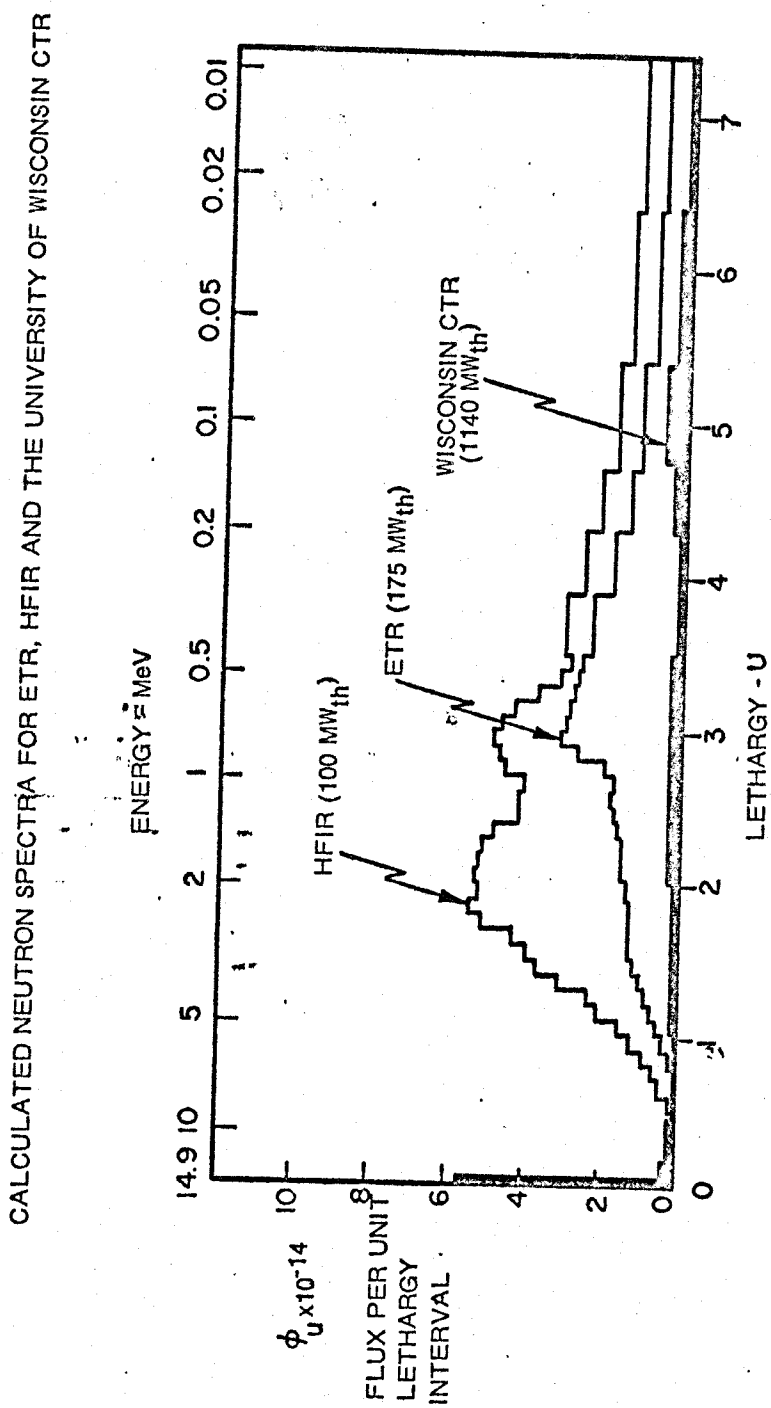
CALCULATED NEUTRON SPECTRA FOR ETR, HFIR AND THE UNIVERSITY OF WISCONSIN CTR
ENERGY - MeV
14.9 10 5 2 1 0.5 0.2 0.1 0.05 0.02 0.01
$\phi_u \times 10^{-14}$
FLUX PER UNIT LETHARGY INTERVAL
10 8 6 4 2 0
HFIR (100 MW$_{th}$)
ETR (175 MW$_{th}$)
WISCONSIN CTR (1140 MW$_{th}$)
0 1 2 3 4 5 6 7
LETHARGY - U

Figure Ia

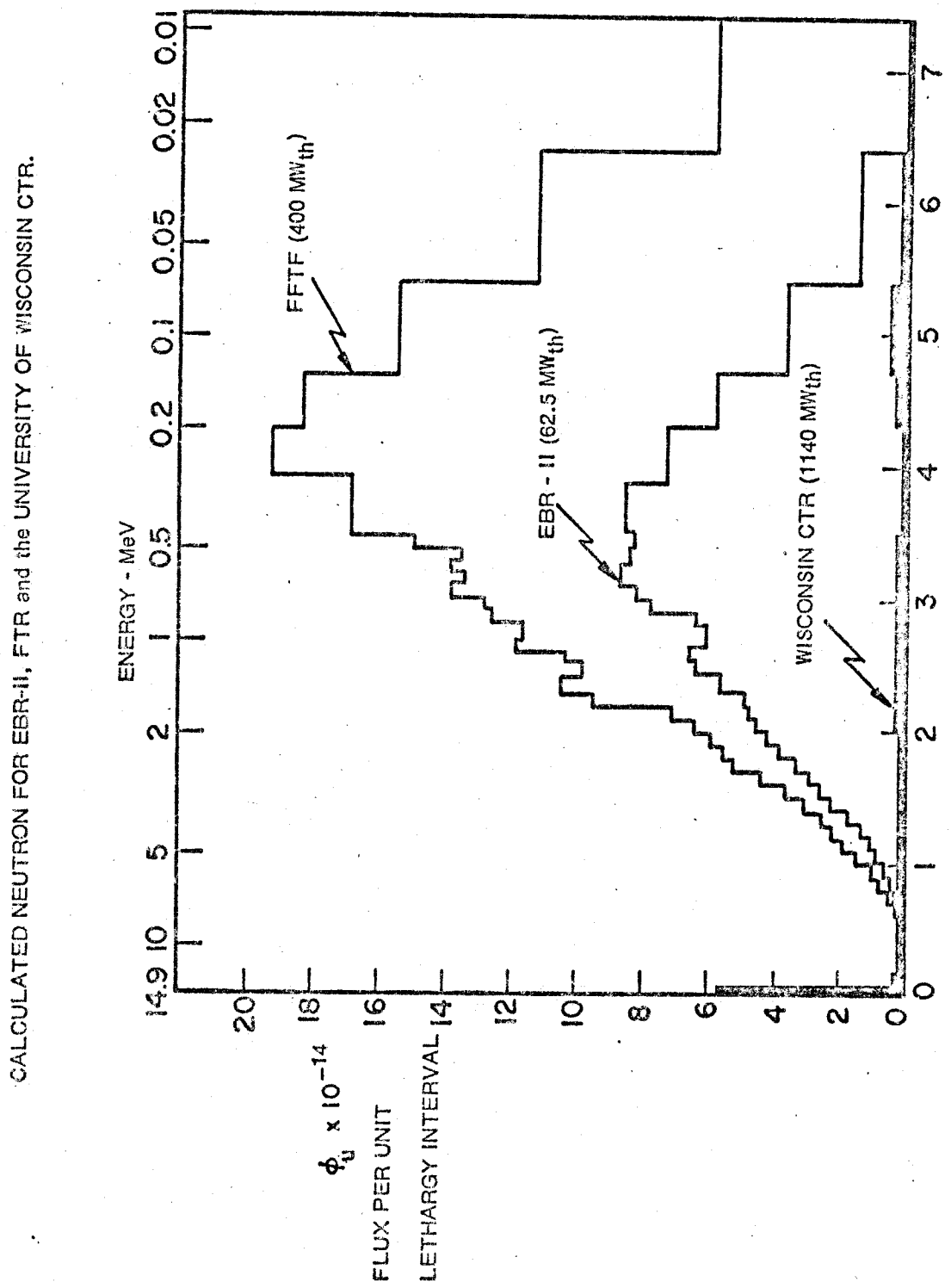
CALCULATED NEUTRON FOR EBR-II, FTR and the UNIVERSITY OF WISCONSIN CTR.
ENERGY - MeV
14.9 10 5 2 1 0.5 0.2 0.1 0.05 0.02 0.01
FFTF (400 MWth)
EBR - II (62.5 MWth)
WISCONSIN CTR (1140 MWth)
FLUX PER UNIT LETHARGY INTERVAL
$\phi_u \times 10^{-14}$
20 18 16 14 12 10 8 6 4 2 0
0 1 2 3 4 5 6 7
LETHARGY - U

Figure 16

particularly the sharp peak 14 MeV, results in a large number of transmutations that have thresholds above the fission spectrum. The characteristic 1/E tail is not seen on the thermal spectra because it is cut off at 10 KeV. Any reaction that has a 1/v cross section may become important in a thermal reactor. The same UWCTR flux spectrum is compared to two fast spectra in Figure Ib. Again the power level is much lower and the flux levels below 7 MeV much higher in the fission reactors. Fast reactor spectra do not exhibit the 1/E thermal tail. However, the average neutron energy of a fast reactor is lower than the average energy calculated for a thermal reactor, ignoring the thermal tail. Fast reactors have a large portion of their flux in the intermediate energy levels, around and just above the resonance region. Fast reactors have enough high energy neutrons to make some reactions that have thresholds in the MeV range important. Resonance reactions are also significant in a fast reactor. It is obvious that measurements made in one type of reactor are of little use to the designer of the other two types.

Cross Sections

There are four major transmutation reactions which may have cross sections large enough to make them important in reactor design. The first is radiative capture, which is primarily important because it may lead to a radioactive nuclide, contributing to the after heat. If the radioactive nuclide produced decays to another

chemical species, it may be an important source of non-gaseous transmutation products. At low energies, (n,γ) cross sections generally have a 1/v dependence, while in the KeV range, some resonance structure is usually observed. The (n,γ) cross section is generally negligible in the MeV range. The second reaction to be considered is the (n,2n) reaction. Like the (n,γ) reaction, this reaction is only important if it leads to a radioactive nuclide. However, the (n,2n) cross section is usually negligible at energies below the MeV range. The third and fourth major reactions are the (n,p) and (n,α) reactions. Charged particle emission results in gas production as well as causing radioactivity and contamination of the metals. Many of the products of (n,p) reactions decay by β^- emission with rather short half lifes, resulting in no appreciable change in the chemical make-up of the material. With some important exceptions, the coulomb barrier prohibits charged particle reactions for neutrons with energies below several MeV. However, there are some light nuclides which exhibit appreciable charged particle emission cross sections at low neutron energies. An important example in the $B^{10}(n,\alpha)$ reaction, which has such a high thermal cross section that it is used to absorb neutrons in thermal reactors.

In addition to these four major transmutation reactions, there are a large number of reactions that can have cross sections large enough to make them important. Charged particle reactions producing

deuterium, tritium and helium-3 may also be important. Also, multiple emissions such as (n,np), (n,nα), (n,3n) and (n,3α) can be important in some materials. Even inelastic scattering can become important if it leads to the creation of a metastable state of the nuclide, which would then decay.

Metastable states of reaction products can be produced through any of the interactions mentioned above. The decay of metastable states can make important contributions to the after heat. In addition, if the metastable states have decay schemes or half lives significantly different than the ground state, they can effect the rate of transmutation in the material. Consideration of metastable states becomes particularly important when considering niobium, because a large number of its isotopes have metastable states. The (n,2n) reaction in Nb^{93} must be handled carefully, because it produces both Nb^{92} and Nb^{92m}. Nb^{92} decays rapidly to zirconium, but Nb^{92m} has a long half life. It has also been shown[2,3] that Nb^{93m} produced through (n,n') reactions in Nb^{93} is an important contributor to after heat.

Although most of the calculations presented in this paper consider only reactions with the nuclides originally present in the natural elements, sequences of reactions are also possible. Experiments in EBR-II have shown that nickel produces large amounts of helium that cannot be explained in terms of the naturally occurring isotopes. It has been postulated[4] that a two step process of the form

$$Ni^{\nu} + n \xrightarrow{\sigma_1\phi_1} I + Y$$

$$I + n \xrightarrow{\sigma_2\phi_2} He + Z$$

is responsible for this anomaulous helium production. The most likely candidate[11] for the intermediate nuclide is Ni^{59}, which could be produced through (n,γ) reactions in Ni^{58}.

Present Understanding of Transmutation Effects

If all of the important cross sections were known and the flux spectrum in a reactor could be specified, the calculation of transmutation rates would be a relatively simple task. Unfortunately, so little data exists for some of the important cross sections that they cannot be quoted with great accuracy. The flux spectrum is also not well-known for most reactors and this limits the accuracy of any calculation.

Low energy and thermal cross sections, which are important in thermal reactors, are fairly well-known. Cross sections in the resonance region have also been studied in considerable detail. However, many of the reactions important in fast reactors and CTR's occur at energies in excess of 1 MeV. The reactions believed to be important for the production of helium in EBR-II are listed in Table I. With the exception of $B(n,\alpha)$, the response range, within which 90% of the helium is produced, is greater than 1 MeV. Because it is difficult to produce high intensity sources of mono energetic, high energy neutrons, very little cross section data is available in this regime. In many cases, the only high

TABLE I–Reference 5

Spectral-Averaged Cross Sections of Materials Irradiated in EBR-II Row 4 Center

Reaction	Helium Concentration and Estimated 2σ Std Dev (atom fraction × 10^6)	Spectral Average Cross Section (mb)			
				Response Range[b]	
		$\bar{\sigma}_m$ (measured)[a]	$\bar{\sigma}_c$ (calculated)	E_L (MeV)	E_U (MeV)
B (n,α)	220 ± 10	170	190	0.017	1.2
Ti (n,α)	< 0.077	< 0.059	-	-	-
V (n,α)	0.021 ± 0.003	0.016	-	-	-
Cr (n,α)	0.13 ± 0.03	0.10	0.061	5.3	12.5
Mn (n,α)	0.11 ± 0.01	0.085	-	-	-
Fe (n,α)	0.097 ± 0.004[c]	0.075	0.051	5.2	12.5
Co (n,α)	0.050 ± 0.003	0.038	0.032	5.8	13.0
Ni (n,α)	1.24 ± 0.06[c]	0.95	0.053	5.5	11.6
Cu (n,α)	0.090 ± 0.005	0.069	0.053[d]	6.1	12.1
Zr (n,α)	0.016 ± 0.001	0.012	-	-	-
304 SS (n,α)	0.32 ± 0.01	0.25	0.19[e]	-	-
N (n,α)	-	-	23.0	1.6	5.6

[a] Calculated from column 2 using Eq. (1) and $\Phi t = 1.30 \times 10^{21}$ n/cm^2. An estimated 10% (1σ) absolute uncertainty is assigned to these measured cross sections, which is due mainly to the uncertainty in the absolute value of Φt. The relative uncertainties between $\bar{\sigma}_m$ values for the different elements is limited only by the uncertainty of the measured helium concentration N_m, column 2.

[b] E_L is the lower and E_U is the upper neutron energy limit, within which 90% of the helium is produced.

[c] The measured nitrogen content of the nickel before and the iron after the irradiation were < 14 ppma and ~22 ppma, respectively; consequently, nitrogen appears to contribute less than 0.001 ppma to the total helium content of the iron and nickel.

[d] Cross section only for the contribution from ^{63}Cu.

[e] Based on the following atom fractions for the 304 SS specimen: Fe(0.72), Cr(0.20), Ni(0.085), B(2.6×10^{-6}), and N(5.5×10^{-3}).

energy data available is for 14 MeV neutron sources, which use the D-T reaction to generate the reactions. Because of the peculiar flux spectrum of the fusion reactor, the cross section for D-T neutrons is quite important. For fast reactors, spectral-averaged cross sections from EBR-II have been reported. A comparison between measured and calculated values of the spectral-averaged cross section for helium production in EBR-II is made in Table I. These measurements of spectral averaged cross sections are limited to a fast spectrum and provide little insight into gas production in a CTR. Until an irradiation facility is devised that will produce a flux spectrum similar to a fusion spectrum, no values of spectral-averaged cross sections for transmutation in a CTR can be measured.

Application of Transmutation Calculations to UWCTR

The general calculational procedure outlined in Figure II was used to generate all of the results presented in this paper. The materials and reactions that were to be considered were fed into the MACK[6] computer code, which read the ENDF/B-III files and calculated the 100 group cross section. The 100 group flux was obtained from a previous calculation. The output from MACK and the results of the neutronics calculations[1] were then fed into a computer program which calculated a total reaction rate per target nucleus, $\sum \sigma g \, \phi g$. The output from this computer program was then used to calculate the production rates of gaseous and non-gaseous production rates and the total amount of radioactivity produced in the system.

Figure II

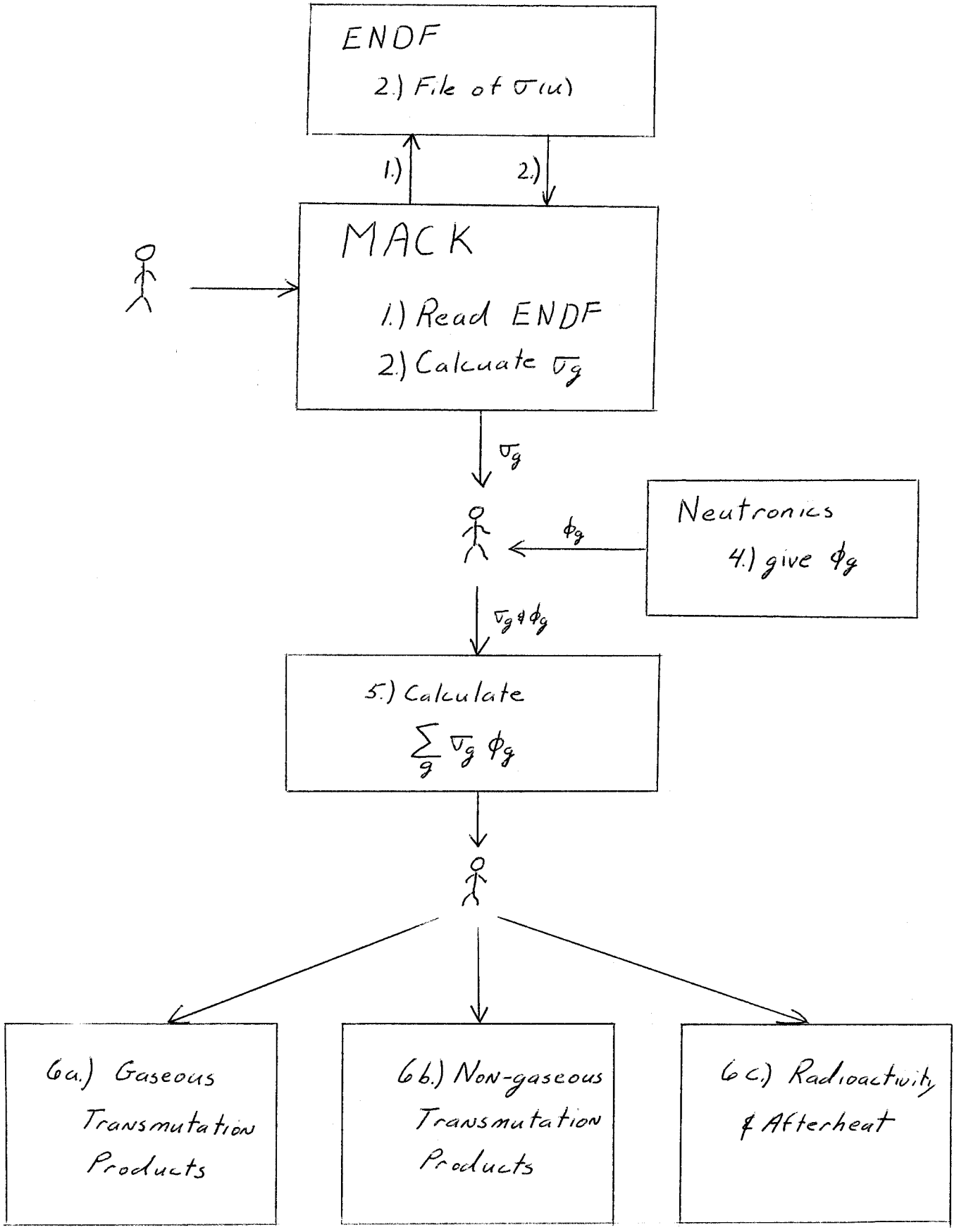
ENDF
2.) File of σ(u)
1.)
2.)
MACK
1.) Read ENDF
2.) Calcuate σg
σg
Neutronics
4.) give φg
φg
σg & φg
5.) Calculate
Σg σg φg
6a.) Gaseous Transmutation Products
6b.) Non-gaseous Transmutation Products
6c.) Radioactivity & Afterheat

Materials and Reactions Considered

Three potential structural materials have been considered, Nb-1Zr, V-20Ti and 316 stainless steel. A typical chemical analysis for commercial purity of each of the alloys has been constructed in Table II. All of the major alloying materials and many of the impurities have been considered. Each of the four major transmutation reactions was considered for all of the materials present. Calculations were only performed for the reactions that seemed to be of major importance and for which data was available. The reactions for which reaction rates were calculated are listed in Table III. Many of the reactions were eliminated because they did not produce chemically different species. Many of the isotopes not considered were only present in small amounts. Also many of the (n,γ) cross sections were ignored because of the complexity of the resonance calculation. A summary of the transmutation reactions not considered is given in Table IV. Because reaction rates were calculated per target nucleus, any combination of the materials included might be considered.

MACK and ENDF/B-III

The raw cross section data for these calculations was taken from ENDF/B-III. These evaluated nuclear data files have been compiled by many different groups from measurements and calculations of cross sections.

Suggested values for the pointwise cross sections $\sigma(u)$ have been formulated for an entire range of energies. All of these evaluated cross sections have been compiled onto the ENDF/B-III tapes.

Table II

Typical Chemical Analyses of Commercial Grade Materials
Parts Per Million by Weight

Element	316 Stainless Steel	Nb-1Zr	V-20Ti
Al	500	<20*	220
As	300*		
B	10	<1	<1
Co	500*	<10*	<10*
Cr	~180,000	<20*	<20*
Cu	1,000	<40*	<40*
Fe	~626,000	<50*	100
Mn	~20,000	<20*	<20*
Mo	~20,000*	<20*	<20*
Nb	500*	~987,000	<50*
Ni	~140,000	<10*	50*
P	200		
S	100*		
Si	7,500	<50	350
Ta	200*	<500	40*
Ti	100	40	~200,000
V	2,000	<20*	~795,000
Zr		~10,000	
C	600	40	150
H		6*	4*
N	100	35	150
O	<200	100	800

*Elements not included

Table III

Transmutation Reactions Considered for These Calculations

Isotopic Abundance-%	Reaction	Important Isotope for 20 Year Plant
100	$Al^{27}(n,2n)$	Mg^{26}
"	$Al^{27}(n,p)$	Al^{27}
"	$Al^{27}(n,\alpha)$	Na^{24}
18.7	$B^{10}(n,\alpha)$	Li^{7}
Total	Cr(n,p)	15% V, 85% Cr
"	Cr(n,2n)	0.2% Ti, 99.8% V
"	$Cr(n,\alpha)$	98% Ti, 2% V
Total	Cu(n,2n)	Ni
"	Cu(n,p)	90% Ni, 10% Cu
"	$Cu(n,\alpha)$	Ni
Total	Fe(n,p)	25% Mn, 75% Fe
"	Fe(n,2n)	98% Mn, 2% Fe
"	$Fe(n,\alpha)$	90% Cr, 10% V
100	$Mn^{55}(n,p)$	Mn
"	$Mn^{55}(n,2n)$	Cr
"	$Mn^{55}(n,\alpha)$	Cr
100	$Nb^{93}(n,2n)$	33% Zr, 67% Nb
"	$Nb^{93}(n,p)$	Zr^{93}
"	$Nb(n,\alpha)$	Zr^{90}
Total	Ni(n,p)	82% Fe, 18% Ni
"	$Ni(n,\alpha)$	68% Mn, 28% Fe, 4% Co
100	$P^{31}(n,p)$	P
"	$P^{31}(n,\alpha)$	Si
Total	Si(n,p)	Si
"	$Si(n,\alpha)$	97% Mg, 3% Si
99.987	$Ta^{181}(n,p)$	Ta^{181}
"	$Ta^{181}(n,a)$	Hf^{178}
99.76	$V^{51}(n,\alpha)$	Cr^{52}
"	$V^{51}(n,p)$	V^{51}
"	$V^{51}(n,\alpha)$	Ti^{48}

Table II (cont.)

Isotopic Abundance-%	Reaction	Important Isotope for 20 Year Plant
51.46	$Zr^{90}(n,p)$	Zr^{90}
"	$Zr^{90}(n,2n)$	Y^{89}
"	$Zr^{90}(n,\alpha)$	Sr^{87}
11.23	$Zr^{91}(n,p)$	Zr^{91}
17.11	$Zr^{92}(n,p)$	Zr^{92}
"	$Zr^{92}(n,\alpha)$	Y^{89} (Sr^{89})
17.4	$Zr^{94}(n,p)$	Zr^{94}
"	$Zr^{94}(n,\alpha)$	Zr^{91}
98.892	$C^{12}(n,\alpha)$	Be^{9}
"	$C^{12}(n,n')$	$3\ He^{4}$
99.635	$N^{14}(n,p)$	C^{13}
"	$N^{14}(n,p)$	C^{14}
"	$N^{14}(n,\alpha)$	B^{11}
99.759	$O^{16}(n,p)$	O^{16}
"	$O^{16}(n,\alpha)$	C^{13}
Total	Ti(n,2n)	8% Sc, 92% Ti
"	Ti(n,p)	Ti
"	Ti(n,α)	21% Ca, 74% Sc, 5% Ti

Table IV

Transmutations Reactions Not Considered for These Calculations

Isotopic Abundance-%	Reaction	Important Isotope for 20 Year Plant
100	$Al^{27}(n,\gamma)$	Si
100	$As^{75}[(n,\gamma),(n,p),(n,\alpha)]$	Se, Ge, As
18.7	$B^{10}[(n,p),(n,T)]$	Be, He
81.3	$B^{11}[(n,p),(n,\alpha),(n,\gamma)]$	B, He, C
100	$Co^{59}[(n,\gamma),(n,p),(n,\alpha)]$	Ni, Fe
4.31	$Cr^{50}(n,\gamma)$	V^{51}
2.38	$Cr^{54}(n,\gamma)$	Mn^{55}
Total	$Cu(n,\gamma)$	Zn
5.84	$Fe^{54}(n,\gamma)$	Mn^{50}
100	$Mn^{55}(n,\gamma)$	Fe^{56}
Total	$Mo[(n,\gamma),(n,p),(n,\alpha),(n,2n)]$	Tc, Ru, Zr, Y
100	$Nb^{93}[(n,np),(n,T)]$	Zr
1.16	$Ni^{64}(n,\gamma)$	Cu^{65}
100	$P^{31}(n,\gamma)$	S
Total	$Si(n,2n)$	Al, Si
Total	$S[(n,\gamma),(n,p)(n,\alpha)]$	Si, Cl
99.987	$Ta^{181}(n,\gamma)$	W^{182}
0.013	$Ta^{180}[(n,p),(n,2n),(n,\alpha)]$	Hf
0.24	$V^{50}[(n,p),(n,2n),(n,\alpha)]$	Ti
11.23	$Zr^{91}(n,\gamma)$	Sr^{88}
17.4	$Zr^{94}(n,\gamma)$	Mo^{95}
98.892	$C^{12}(n,p)$	C^{12}
	$C^{12}(n,2n)$	B^{11}
0.108	$C^{13}[(n,p),(n,\alpha)]$	C, Be
0.365	$N^{15}[(n,\ ),(n,p),(n,\alpha)]$	O, N, C
99.759	$O^{16}(n,2n)$	N^{15}
0.037	$O^{17}[(n,p),(n,\gamma)]$	O, C
0.204	$O^{18}[(n,\gamma),(n,p),(n,\alpha)]$	F, O, N

Without a computer code to read them, the ENDF/B-III tapes are unmanageable. The MACK computer code developed by Abdou, Maynard and Wright,[6,22,23] processes the ENDF/B-III tapes. MACK was designed to calculate neutron kerma factors for energy deposition in materials, but also has the ability to calculate group cross sections. The weighting function used for these calculations was a constant flux value over the lethargy interval. Cross sections for which the ENDF/B-III tapes were not available were taken from BNL-325. Titanium cross sections were taken from ANL-7387.

Neutronics

The neutronics calculations for the UWCTR were made by Maynard and Abdou.[1] The one dimensional, homogenized system shown in Figure III was used for these calculations. The flux spectrum was calculated at 169 different positions in the reactor. The six positions shown in Figure III were selected for calculating reaction rates. At this time, only the data from position 1 in the first wall has been calculated. The first wall is subjected to the highest fluences and will probably undergo the greatest changes. Although this flux spectrum was obtained for a stainless steel structure, it will be used for considering several different materials.

Gas Production

The calculation of helium and hydrogen production rates does not require that every isotope of an element be considered separately. Most of the gas production in the structural materials comes from

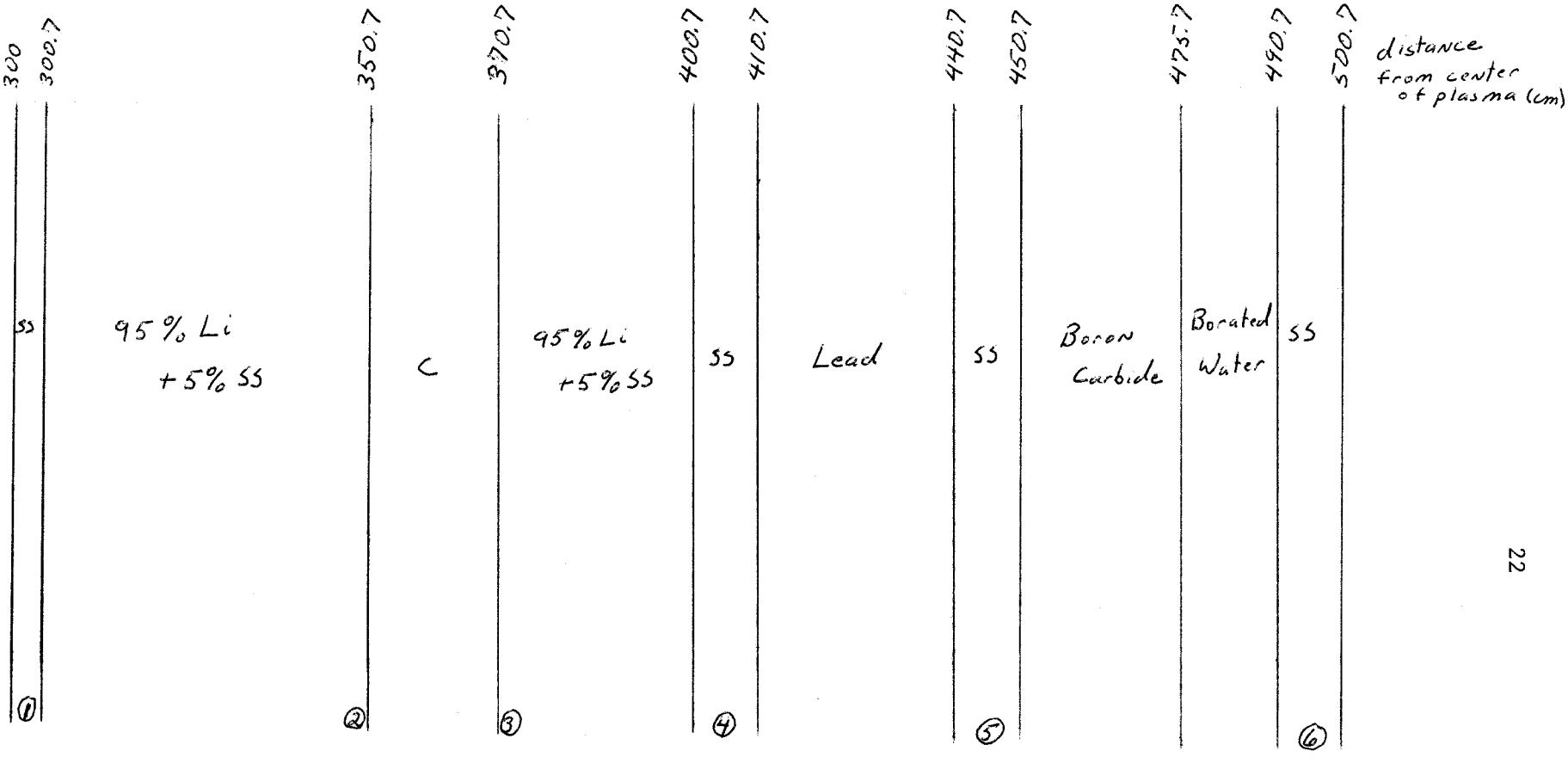

Ⓟ ... six positions considered for these calculations

Figure III

(n,p) and (n,α) reactions. There is an (n,3α) reaction in carbon that can become important in materials that contain appreciable amounts of carbon. Many of the (n,D) and (n,T) reactions, which are also responsible for hydrogen production have been ignored. Gas production rates have been calculated in $\frac{\text{appm}}{\text{MW/m}^2 \text{ year}}$ which will be referred to as an amy. The gas production rate for any element is then

$$\begin{pmatrix}\text{amys of}\\ \text{gas produced}\\ \text{in structure}\end{pmatrix} = \begin{pmatrix}\text{appm of}\\ \text{element}\\ \text{present}\end{pmatrix}\left(\sum_g \sigma_g \phi_g\right)\left(\frac{3.1536 \times 10^7 \text{sec}}{\text{year}}\right)$$

where the flux is normalized to a wall loading of MW/m^2. The production of helium from Ni^{59} may be important, but it has not been considered in these calculations.

Non-Gaseous Transmutation Products

Different isotopes of the same element may have widely varying nuclear properties. A (n,p) reaction in Fe^{56} produces Mn^{56} while a (n,p) reaction in Fe^{54} produces Mn^{54}. Manganese-56 decays by β^- emissions back into Fe^{56} with a half life of 2.6 days producing no net change in the material composition. However, Mn^{54} decays by electron capture to Cr^{54} with a half life of 303 days, producing a change in the material composition. Often, the only cross section data available was for the natural element. When this was the case, the reactions were divided up on the basis of the isotopic abundance and the 14 MeV cross section taken from BNL-325. The fraction, f, of the total reaction rate was calculated from the formula

$$f = \frac{\left(\begin{matrix}\%\text{ abundance of} \\ \text{isotope}\end{matrix}\right)\left(\begin{matrix}14\text{ MeV x-section} \\ \text{of isotopes}\end{matrix}\right)}{100\left(\begin{matrix}14\text{ MeV x-section} \\ \text{of element}\end{matrix}\right)}$$

This value for f should be reasonable as long as most of the reactions take place in the highest energy group. The large spike in the flux spectrum at 14 MeV is responsible for most of the reactions. The production rates for non-gaseous transmutation products can then be calculated analagously to the gas production rates.

$$\left(\begin{matrix}\text{amys of} \\ \text{product}\end{matrix}\right) = f\left(\begin{matrix}\text{appm of} \\ \text{element}\end{matrix}\right)\left(\sum_g \sigma_g \phi_g\right)\left(\frac{3.1536\text{ sec}}{\text{year}}\right)$$

Only reaction products that had half lives of greater than twenty years were considered as important in the reactor system.

Radioactivity and After Heat

Calculations of radioactivity in the reactor are quite complicated because the amount of each radioactive nuclide present in the reactor must be traced throughout the life of the reactor and after shut down. In making these calculations, many cross sections that were not important to the previous calculations become extremely important. In particular, cross sections for radioactive nuclides may become important. In order to make calculations for a reactor constructed of pure niobium, Steiner[3] has presented a list of assumptions about the unknown cross sections. A list of these assumptions is given in Table V to illustrate the

Table V

Assumptions About Cross Sections Used to Calculate After Heat in Niobium - Reference 3

*1. $Nb^{93}(n,2n)$ from ENDF/B III

2. 17.7% of $Nb^{93}(n,2n)$ produce Nb^{92n}

3. 83.3% of $Nb^{93}(n,2n)$ produce Nb^{92}

4. $Nb^{94}(n,2n)Nb^{93m} = Nb^{93}(n,2n)Nb^{92m}$

5. $Nb^{92}(n,2n)Nb^{91m} = Nb^{93}(n,2n)Nb^{92m}$

6. $Nb^{94}(n,2n)Nb^{93} = Nb^{93}(n,2n)Nb^{92}$

7. $Nb^{92}(n,2n)Nb^{91} = Nb^{93}(n,2n)Nb^{92}$

8. $Nb^{91}(n,2n) = 0$

9. $Nb^{95}(n,2n) = 0$

*10. $Nb^{93}(n,n')$ from ENDF/B III

11. 20% of $Nb^{93}(n,n')$ produced Nb^{93m}

12. Nb^{91}, Nb^{92}, $Nb^{94}(n,n')$ same as $Nb^{93}(n,n')$

13. $Nb^{95}(n,n') = 0$

*14. $Nb^{93}(n,\gamma)$ as in ENDF/B III

15. 90% of $Nb^{93}(n,\gamma)$ produce Nb^{94m}

16. $Nb^{94}(n,\gamma) = 15 \times Nb^{93}(n,\gamma)$

17. 90% of $Nb^{94}(n,\gamma)$ produce Nb^{95m}

18. Nb^{91}, Nb^{92} and $Nb^{95}(n,\gamma) = 0$

19. all other reactions ignored [(n,α), (n,p), etc.]

*Assumptions based on measured cross sections

problems in making this calculation. Of all the materials considered, the radioactivity problems in niobium are probably the best understood.

It is important to realize that the best calculational procedures are still limited by the accuracy of the data. The calculations presented here have been carried out by Vogelsang and Sung[2] for the UWCTR. The calculations are only preliminary and will be improved as better data becomes available. A computer program has been written to take the cross sections and fold them into the flux spectrum at a number of different regions in the reactor. This program then calculated the amount of radioactivity produced in the entire reactor volume.

RESULTS

V-20Ti

The calculation of gas production in V-20Ti is summarized in Tables VI and VII. Helium is produced at 71.8 amys in the V-20Ti structure. The major producer of helium is the vanadium (88%) while titanium contributes much less helium per metal atom contributing only 6% of the total helium production. The impurities (most notably carbon at 2.3% and oxygen at 1.3%) produce the remaining 6% of the helium.

The total hydrogen production rate in V-20Ti is 219.3 amys. More than 99% of the hydrogen is produced in the major alloy components, V and Ti. Titanium produces a larger amount of hydrogen per metal atom, 47%, than the vanadium which contributed 52% of the total hydrogen production.

The major metallic transmutation reactions in V-20Ti involve V, T, Cr and Sc. The chromium produced by (n,γ) reactions in V^{51} may be the most important. The production rate for each of these metals is presented in Table VIII.

The effects of a small addition of Cr to V-20Ti are not well-known. However, Cr is used in larger quantities as an alloying material in some V-Ti systems. Twenty years of operation of UWCTR would produce 0.1 atomic percent Cr while a reactor operating at 10 MW/m^2 would produce 2 atomic percent Cr. Both of these numbers represent substantial increases in the intital concentration of Cr.

Table VI

Gas Production Rates in Potential CTR Materials

	appm/MW/m^2/year		appm in 20 Years 0.5 MW/m^2 UWCTR		10 MW/m^2	
Alloy	He	H	He	H	He	H
V-20Ti	71.8	219.3	718	2193	14,360	43,860
Nb-1Zr	36.2	113.8	362	1138	7,240	22,760
316 SS	278.7	636.5	2787	6365	55,740	127,300

Table VII

Major Contributors to Gas Production in Potential CTR Materials

Alloy	Host Metal	% Contribution: Major Alloying Agent	% Contribution: All Impurities
		HELIUM	
V-20Ti	88	6 (Ti)	6 (C-2.9%)
Nb-1Zr	96	0.3 (Zr)	3.7 (C-2.8%)
316 SS	72	16 (Cr) 2.3 (Ni)	9.7 (Si-4.5%) (C-3.3%)
		HYDROGEN	
V-20Ti	52	47 (Ti)	<1 (Si-0.3%)
Nb-1Zr	98	1 (Zr)	<1 (Si,N-0.2%)
316 SS	49	13(Cr) 34(Ni)	4 (Si-2.8%)

Table XVII

Major Metallic Transmutation Reactions in

in Potential CTR Materials

	Element	Production Rate appm/MW/m^2/yr.	after 20 yrs. UWCTR Atomic %	% Change(a)	20 years at 10 MW/m^2 At. % of Alloy	% Change(a)
V-20Ti	V	- 162	-0.162	- 0.2	- 3.24	-5.18
	Cr	+ 99	+0.099	+260	+ 1.98	+5200
	Ti	+ 53	+0.053	+ 0.27	+ 1.06	+5.3
	Sc	+ 9.1	+0.0091	NA	+ 0.18	NA
Nb-1Zr	Nb	-1485	-1.485	- 1.48	-29.6	-29.5
	Zr	+1473(b)	+1.473	+147	+29.4	+2940
	Y	+ 11.7	+0.0117	NA	+ 0.234	NA
316 SS	Fe	-1224	-1.224	- 1.96	-24.5	-39.1
	Cr	+ 24	+0.024	+ 0.13	+ 0.48	+ 2.7
	Ni	- 177	-0.177	- 1.26	- 3.54	-25.3
	Mn	+1160	+1.160	+ 58.0	+23.20	+1150
	V	+ 177	+0.177	+ 80.0	+ 3.54	+1600
	Ti	+ 45	+0.045	+390	+ 0.9	+7800

(a)based on original composition

(b)no burn out included

NA-Not Applicable

Titanium is also produced at a modest rate. In the most extreme case of 10 MW/m^2, only 1 atomic percent Ti is produced after 20 years. When compared to the original 20 atomic percent of titanium, the increase in titanium is probably not important. However, the addition of 1 atomic percent Ti to a structure of pure vanadium might be important. The mechanical properties of vanadium-titanium alloys at room temperature as a function titanium content are shown in Figure IV.[9] An extremely brittle alloy might be formed from a first wall of pure vanadium.

Nb-1Zr

Of the three materials considered, Nb-1Zr has the lowest gas production rates for both helium and hydrogen. Although the impurity atoms produce relatively large amounts of gas per atom, the niobium is responsible for 96% of the helium and 98% of the hydrogen produced in the first wall.

The (n,2n) cross section in Nb^{93} is large (1.180 barns) and ~1/3 of those reactions lead to the production of Zr^{92}. The amount of Zr produced is large enough that the burn-up of the new zirconium becomes appreciable, but it is not included in this report. According to Figure V,[10] the ductility at 100° C of the original Nb-1Zr alloy may be decreased by a factor of three with the addition of 4% Zr to the system. As shown in Figure VI, the Nb-Zr system undergoes a phase change at ~10-15%. This phase change represents an upper limit to the amount of Zr that can be tolerated in the Nb. The first wall of a reactor operating at 10 MW/m^2 would reach this 10%

Figure IX

Effect of Titanium on Room Temperature Mechanical Properties of Vanadium

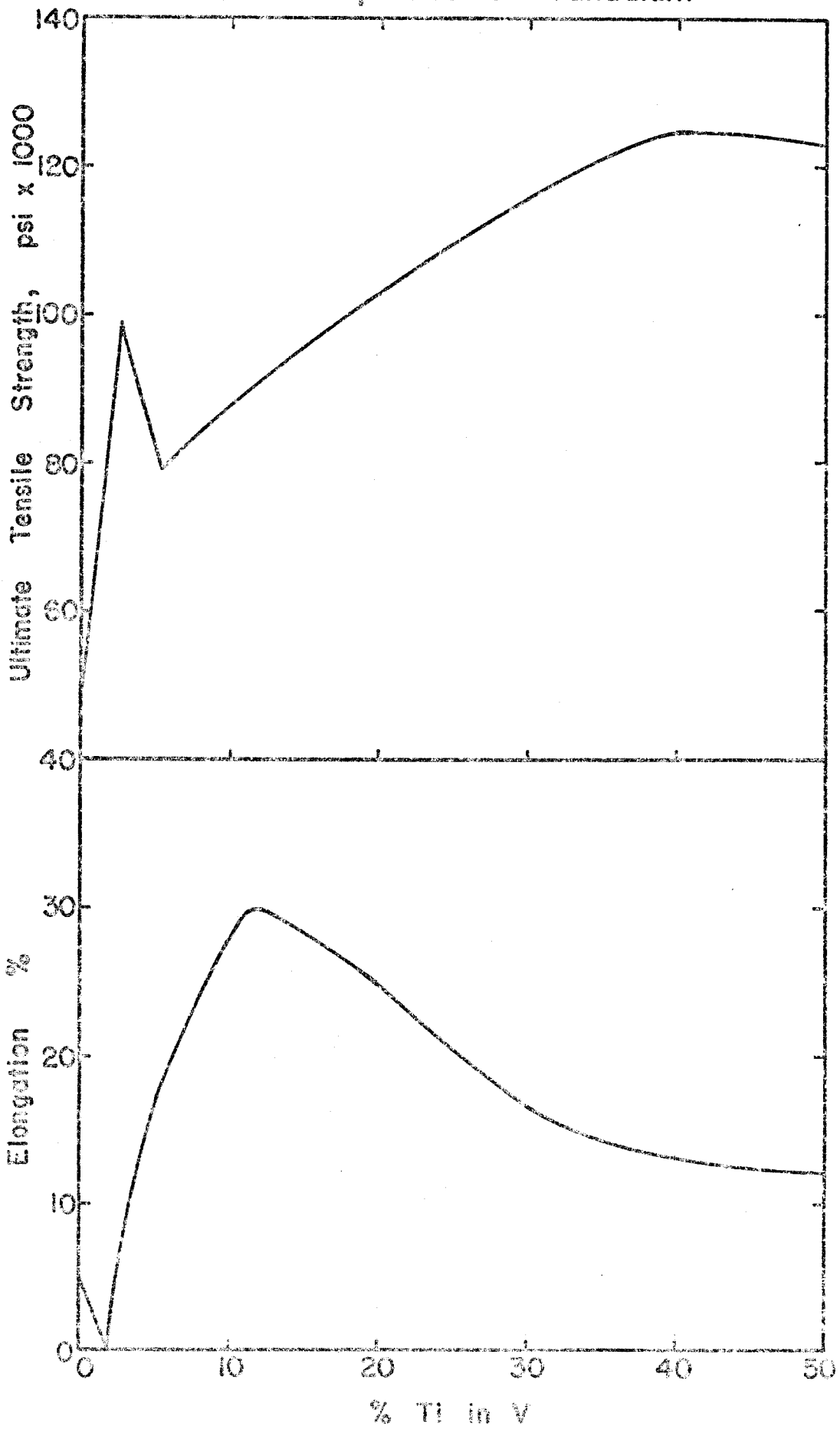

Figure Ⅳa

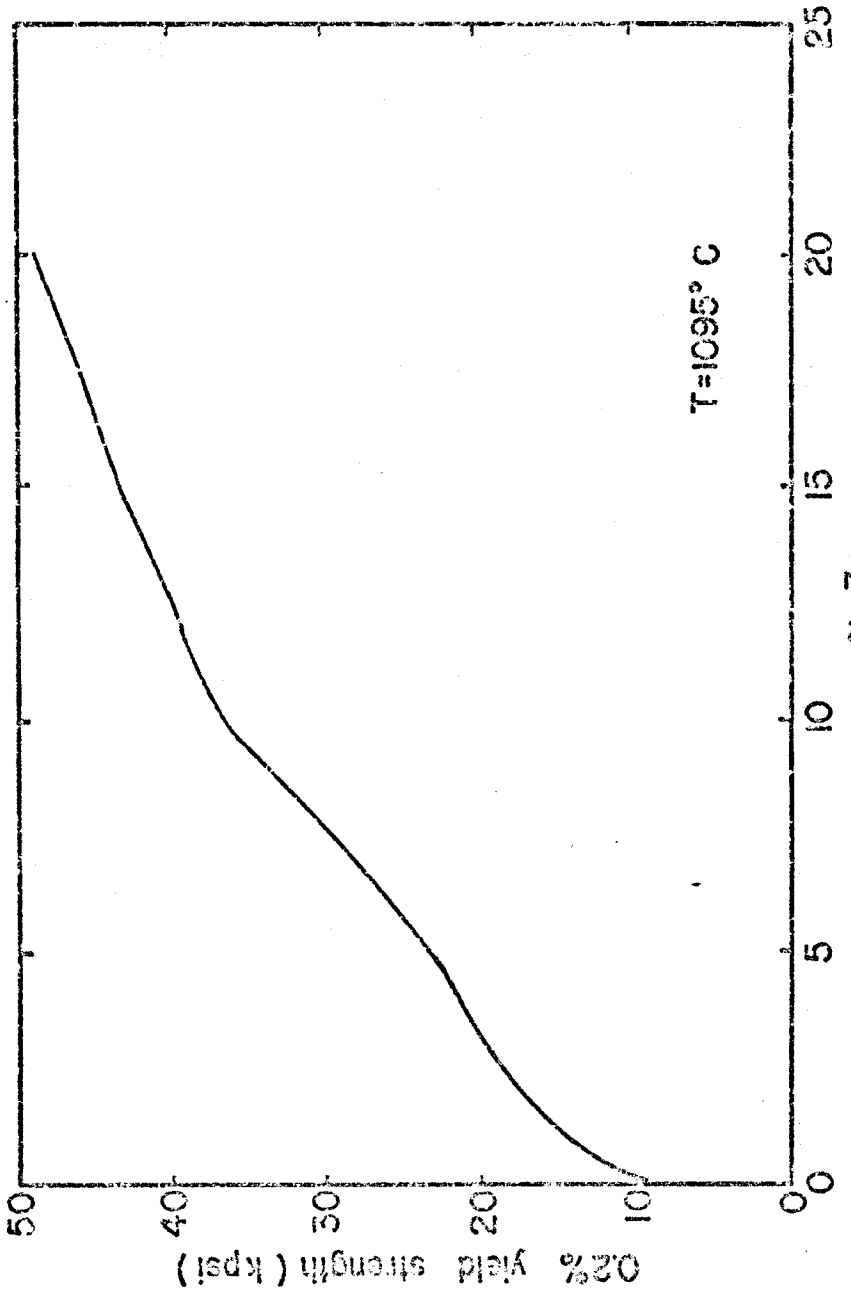

Effect of Zirconium on the Yield Strength of Niobium

Figure Vb

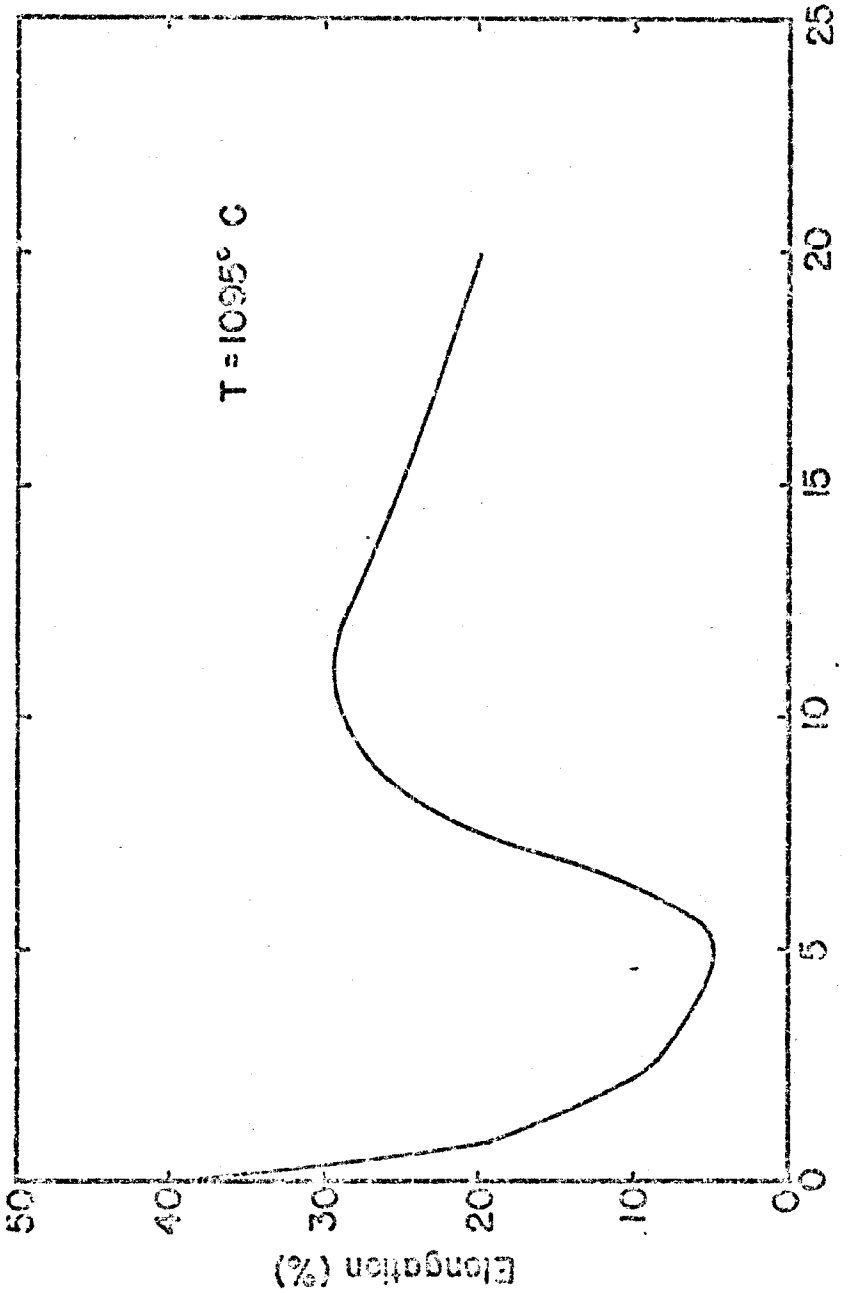

Effect of Zirconium on Ductility of Niobium

Figure XI

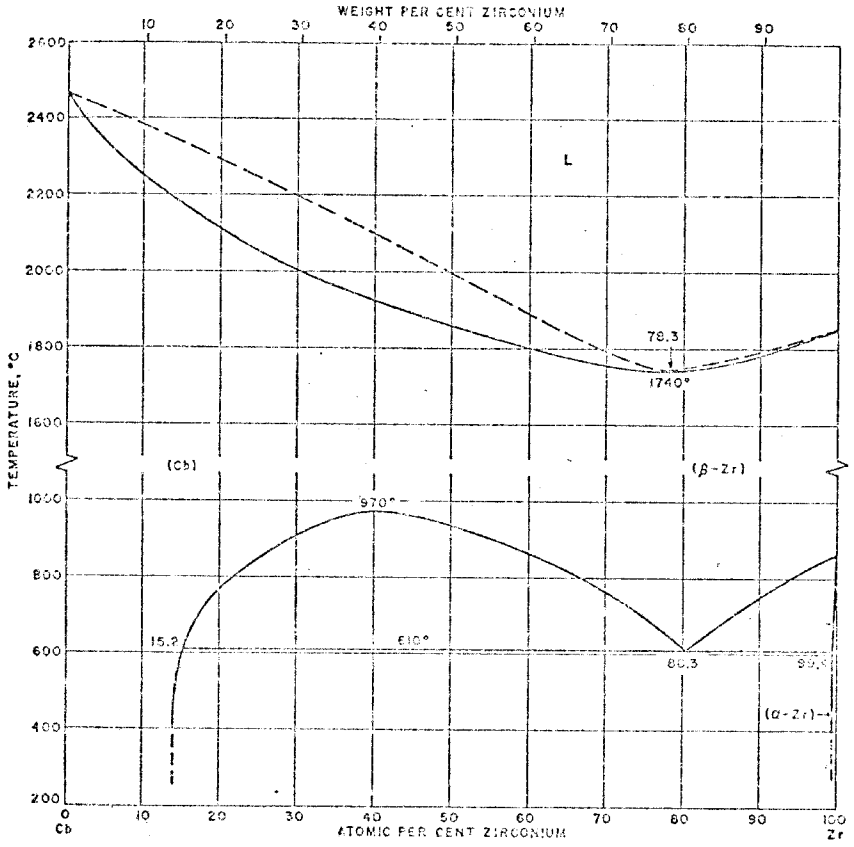

Niobium-Zirconium Phase Diagram

limit in 6 years. The only other non-gaseous transmutation product produced in appreciable amounts is yittrium, which will probably not be important.

316 Stainless Steel

316 stainless steel produces helium at a rate 4 times as fast as V-20Ti and 8 times as fast as Nb-1Zr. Even with the low wall loading of the University of Wisconsin design, helium will be produced at the rate of 147 appm/year. This helium production rate is almost 10 times that obtained in the core of EBR-II operating at 50 MW.[7] The bulk of the helium (72%) produced in stainless steel comes from iron while Cr is responsible for an additional 16%. Ni, Si and C also produce appreciable amounts of helium. The (n,α) cross section in Fe^{56} is the primiary producer of helium stainless steel. This cross section is extremely difficult to measure because it leads to the production of Cr^{58} which is stable. The values of the natural iron (n,α) cross section in ENDF/B-III seem to be based on calculations of the Fe^{56} (n,α) cross sections. If these calculations over-estimate the cross section, the helium production rates calculated here are also an over-estimate. Stainless steel also produces more hydrogen than the other materials considered. Iron only produces half the total amount of hydrogen. Nickel and chromium account for most of the remaining hydrogen production.

Stainless steel is a complex alloy and the effects of changes in composition are hard to evaluate. The AISI composition ranges for some typical 300 series stainless steels are given in Table IX.

Table IX

AISI Standard Composition Ranges

For 300 Series Stainless Steels

	Weight %					
AISI Type	C	Si	Mn	Ci	Ni	Mo or Nb
304	0.08	<1	<2	18-20	8-12	-
316	0.08	<1	<2	16-18	10-14	2-3 (Mo)
321	0.08	<1	<2	17-19	9-12	-
347	0.08	<1	<2	17-19	9-13	0.8(Nb)

The most important metallic transmutation product in stainless steel is manganese. If the original Mn concentration is 2%, the UWCTR reactor would produce 58% of the original concentration in its 20 year life. However, a reactor operating at 10 MW/m^2 would double its original Mn concentration in less than 2 years. A reactor operating at 10 MW/m^2 may also burn out enough nickel or produce enough vanadium to change the composition of the steel. 20 years of irradiation in a reactor operating at 10 MW/m^2 might change a 300 series steel into a 200 series steel with a very high Mn content. Manganese is an austenite stabilizer and would probably keep the steel from becoming ferritic which must be a primary concern. The effects of high Mn concentrations on stainless steel are not known.

Radioactivity and After Heat

The amounts of radioactivity and after heat present in the entire UWCTR system as a function of time after shut down for several different operating times have been calculated by Vogelsang and Sung.[2] The preliminary results of their calculations are shown in Figures VII and VIII. A reactor operating at 1000 MW_{th} would produce 3000 megacuries in a Nb structure at shut down. The level of radioactivity falls off as the Nb^{92m}, Nb^{94m} and Nb^{95m} decay away and at 200 years, the level of radioactivity is approximately nine megacuries. Stainless steel has an initial radioactivity level of 1000 megacuries which is mostly Fe^{55}. After 200 years, the total activity is less than one megacurie. The initial radioactivity of the vanadium structure is 650 megacuries.

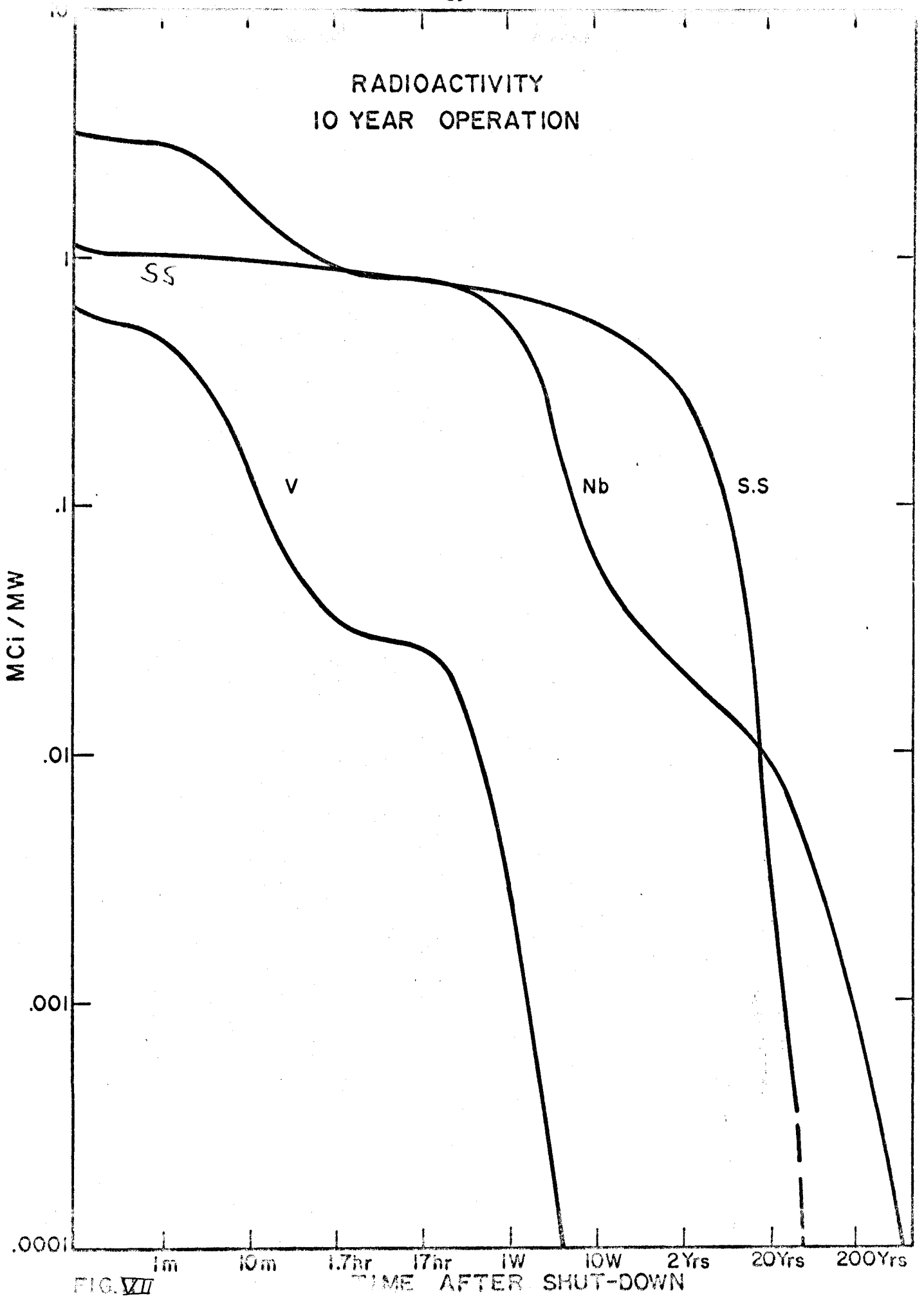
RADIOACTIVITY
10 YEAR OPERATION
SS
V
Nb
S.S
MCi / MW
1
.1
.01
.001
.0001
1m
10m
1.7hr
17hr
1W
10W
2Yrs
20Yrs
200Yrs
TIME AFTER SHUT-DOWN

FIG. VII

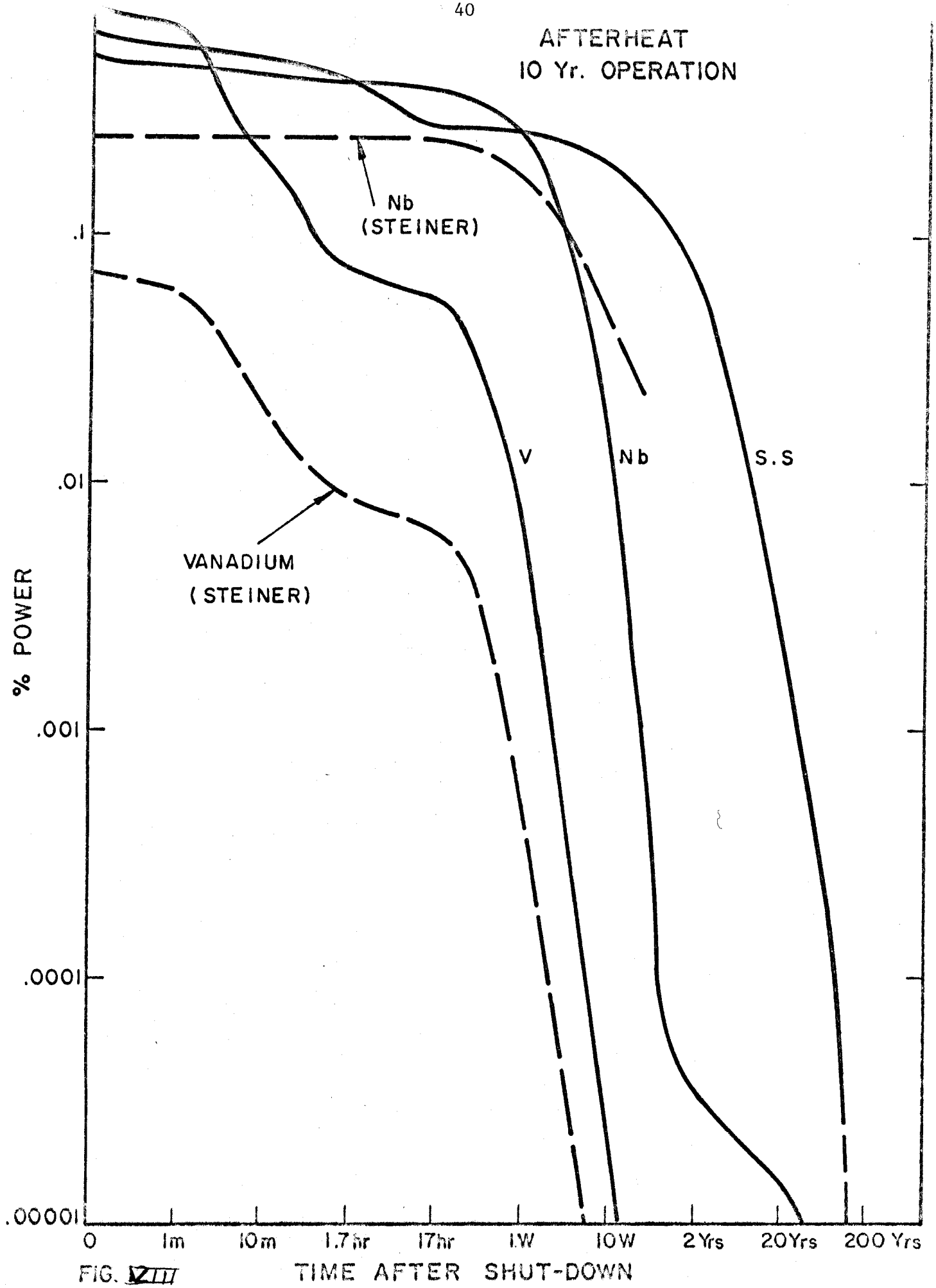
AFTERHEAT
10 Yr. OPERATION
Nb
(STEINER)
V
Nb
S.S
VANADIUM
(STEINER)
% POWER
.1
.01
.001
.0001
.00001
0
1m
10m
1.7hr
17hr
1W
10W
2Yrs
20Yrs
200 Yrs
TIME AFTER SHUT-DOWN

FIG. XIII

The radioactive isotopes produced in vanadium are relatively short lived and the total amount of radioactivity falls off to very low levels within two years. The initial levels of radioactivity in any of these materials would prohibit any direct maintenance of the reactor system. In analyzing the accident potential of the system, it is important to know what isotopes are present as well as the total amount of curies. A good example of this problem is Sr^{89}, which is not present in large enough quantities to be considered in the calculations of total radioactivity, but has chemical properties which may make it important to a safety analysis. A good indication of the importance of each isotope is the maximum allowable number of curies per cubic centimeter of water. A further discussion of this problem will be found in Appendix A.

The after heat generated by radioactive decay of the structural material is also important to reactor design. The after heat results from the deposition of energy in the material by the reaction products. If all of the reaction products are stopped within the reactor, the energy deposited will be the decay energy of the radioactive nucleus. However, in β decay a large portion of the energy will be carried out of the reactor by a neutrino. The average energy deposited in the reactor by a β particle is approximately 30% of the total decay energy. In the calculation of after heat, an average energy deposited in the reactor by each type of decay is included. A summary of the after heat calculation is shown in Figure VIII. The after heat is quoted in terms of percent of operating power. Although the initial number of decays per second

in vanadium is the lowest of the three materials considered, the initial after heat of vanadium is the highest. The after heat falls off after shutdown at approximately the same rate as radioactivity. Again, the afterheat of vanadium falls off much faster than either niobium or stainless steel.

Conclusion

Even for the UWCTR reactor with a relatively low wall loading, the helium production rates are very high. Nb-1Zr has the lowest gas production rates for both hydrogen and helium. V-20Ti produces twice as much gas as the Nb-1Zr, but it is still low compared to the gas produced in the stainless steel.

There appears to be no metallic transmutations that severely limit the performance of V-20Ti. Niobium-1% Zr is limited by the production of Zr in the system and would probably be unsatisfactory for a reactor operating at 10 MW/m^2. It is hard to specify any limits for transmutation products in stainless steel, but a reactor operating at 10 MW/m^2 would produce large amounts of manganese. The loss of nickel and the production of vanadium may also limit the performance of 316 stainless steel. On the basis of these results, V-20Ti would appear to have the best nuclear properties. The gas production rate for V-20Ti is of the same order of magnitude as the Nb-1Zr gas production rate. There are no major metallic transmutation problems in the vanadium system. The most important consideration may be the short lived radioactivity that is produced in a vanadium system. A reactor structure built with vanadium would not have as many difficult radioactive waste storage problems as the other materials considered.

Several areas for further study might be suggested. This calculation could be improved by considering some or all of the reactions listed in Table IV, as well as extending the number of

materials included. Other alloys, such as the Vanstar series might be considered. The calculation might be refined to consider the effects of burn out on the production of the major metallic transmutation products. The data is also available to extend the calculations of transmutation rates to other portions of the reactor. The carbon in the graphite reflector may also exhibit important transmutation effects which have not been considered here. Many of the cross sections used in this calculation are not well-known and need to be studied more closely. One cross section that is particularly important is the Fe (n,α) cross section. The effect of Ni^{59} on the helium production rates should also be included when the data becomes available. Finally, the effect of transmutations on the mechanical properties of the materials need to be considered. The effects of helium production in reactor materials on void formation and ductility are presently being studied. Before a CTR can be built, the mechanical properties of the alloys being produced through transmutations will have to be studied.

APPENDIX A

The total amount of curies present in a reactor is not an adequate measure of the potential biological hazard. Curie for curie, some radioactive species are more dangerous than others. One measure of the biological hazard is presented by any nuclide is its maximum permissible concentration (mpc) in air. To assess the biological hazard of any reactor, Steiner[8] has suggested using the total number of curies of each radioactive species present divided by the maximum permissible concentration in air.

In examining the reaction products of Nb-1Zr system, it was noticed that the (n,α) reaction in Zr^{92} produces Sr^{89}. Even though Nb^{75} is the major source of radioactivity in the system, the mpc of Sr^{89} in air is 1000 times smaller than the mpc of Nb^{95} in air. The equilibrium amount of Sr^{89} in the first wall may be calculated by equating the decay rate and production rate of Sr^{89}.

$$\lambda_{89} N_{89} = N_{92} \sigma_{92} \phi$$

where

λ_{89} = decay constant for Sr^{89}
N_{89} = number of Sr^{89} atoms
N_{92} = number of Zr^{92} atoms
σ_{92} = (n,α) cross section for Zr^{92}
ϕ = flux at first wall

However, the build up of zirconium in the Nb-1Zr system is due almost entirely to an increase in Zr^{92}. When this build up is included, the equilibrium number of curies of Sr^{89} in the first wall of the UWCTR operating at a wall loading, M (in MW/m^2), at

time t (in years) is given by the formula

$$Sr^{89} \text{ Curies} = 15{,}120\ M\ [1.711 + 1.24\ t\ M]$$

At long times and high wall loadings, the original Zr^{92} becomes less important and the Sr^{89} activity in the UWCTR first wall as a function of time is plotted in Figure IX for wall loadings of 0.5 and 10 MW/m^2. Although the activity of Sr^{89} in the system is low compared to the overall activity of the system, the biological hazard may be comparable to that of the tritium.

This is only one of many radioactive products that may exist in small amounts, but be very important to an analysis of the biological hazard potential of a reactor. High wall loadings may make many other two step processes important. A thorough analysis of the system might reveal more potentially dangerous species. Such an analysis should certainly be made.

REFERENCES

1. M. A. Abdou et. al., "Preliminary Conceptual Design of a Tokamak Reactor," to be published in Proceedings of Texas Symposium on the Technology of Controlled Thermonuclear Fusion Experiments and the Engineering Aspects of Fusion Reactors.

2. W. A. Vogelsang and T. Sung, personal communication.

3. D. Steiner, "The Neutron-Induced Activity and Decay Power of the Niobium Structure of a D-T Fusion Reactor Blanket," ORNL-TM-3094, (1970).

4. J. Weitman, N. Daverhog, S. Farvolden, "Anomalous Helium Production in Nickel," Trans. Am. Nucl. Soc., 13, 557, (1970).

5. W. N. McElroy, H. Farrar IV, and C. H. Knox, "Helium Production Cross Sections for Elements Irradiated in EBR II," Trans. Am. Nucl. Soc., 13, 314, (1970).

6. M. A. Abdou, C. W. Maynard and R. Q. Wright, "MACK: A Program to Calculate Neutron Energy Release Parameters (Fluence-to-Kerma Factors) and Multigroup Neutron Reaction Cross Sections from Nuclear Data in ENDF Format," ORNL-TM-3994 (1973).

7. W. N. McElroy, H. Farrar IV, "Helium Production in Stainless Steel and Its Constitutents as Related to LMFBR Development Programs," HEDL-SA-193, (1971).

8. D. Steiner, "Preliminary Observations on the Radiological Implications of Fusion Power," Nuclear Safety, 13, 353, (1972).

9. W. Rostoker, The Metallurgy of Vanadium, New York: John Wiley and Sons, Inc., (1958).

10. F. T. Sisco and E. Epremian, Colombium and Tantalum: New York John Wiley and Sons, Inc., (1963).

11. A. A. Bauer and M. K. Drake, "Helium Generation in Stainless Steel and Nickel," JNM, 42, 91-95, (1972).

12. D. J. Dudziak, "Discrete-Ordinate Neutronic Analysis of a Reference Theta-Pinch Reactor," LA-DC-72-1427, (1972).

13. D. Steiner, "The Nuclear Performance of Fusion Reactor Blankets," Nuclear Appl. & Tech., 9, 83, (1970).

14. D. J. Dudziak, "A Technical Note on D-T Fusion Reactor After Heat," Nuclear Technology, 10, 391, (1971).

15. D. Steiner, "Long-Lived Activities and Radioactive Waste Management Associated with D-T Fusion Reactors," FRT-MEMO-71(1), (1971).

16. L. A. Booth, "Control Station Power Generation by Laser-Driven Fusion," LA-4858-MS,Vol. I, (1972).

17. T. E. Scott, "Hydrogen Embrittlement and Other Effects in Thermonuclear Reactor Materials," to be published.

18. J. Weitman, N. Daverhog and S. Farvolden, "Helium Production in Fe, Cr, Ni, Ti and Cu due to Fission Neutron Part of Reactor Spectra," Trans. Am. Nucl. Soc., 13, 558, (1970).

19. N. D. Dudey, S. D. Harkness and H. Farrar IV, "Helium Production in EBR-II Irradiated Stainless Steel," Nucl. App. and Tech., 9, 700, (1970).

20. B. A. Hutchins, J. E. Turner, H. Busboom and F. A. Compielli, "Helium Generation in Metals Irradiated in EBR II," Trans. Am. Nucl. Soc., 12, 587, (1969).

21. A. L. Ward and J. J. Holmes, "Ductility Loss in Fast Reactor Irradiated Stainless Steel," Nucl. App. and Tech., 9, 771, (1970).

22. M. A. Abdou and C. W. Maynard, "MACK: A Progeam to Calculate Neutron Energy Release Parameters and Multigroup Neutron Reaction Cross Sections from ENDF/B," to be presented at the Am. Nucl. Soc. Meeting, June 1973.

23. M. A. Abdou and C. W. Maynard, "A Library of Multigroup Kerma Factors and Partial Cross Sections for Fusion Neutronics and Photonics," to be presented at the Am. Nucl. Soc. Meeting, June 1973.

24. E. M. Pennington and J. C. Gajniak, "Compilation of ENDF/B Data for Magnesium, Titanium, Vanadium, Molybdenum and Gadolinium," ANL-7387,(1968).

25. M. S. Allen, M. K. Drake, "Neutron Cross Sections for Niobium AEC Research and Development Report, GA-8133, (1967).

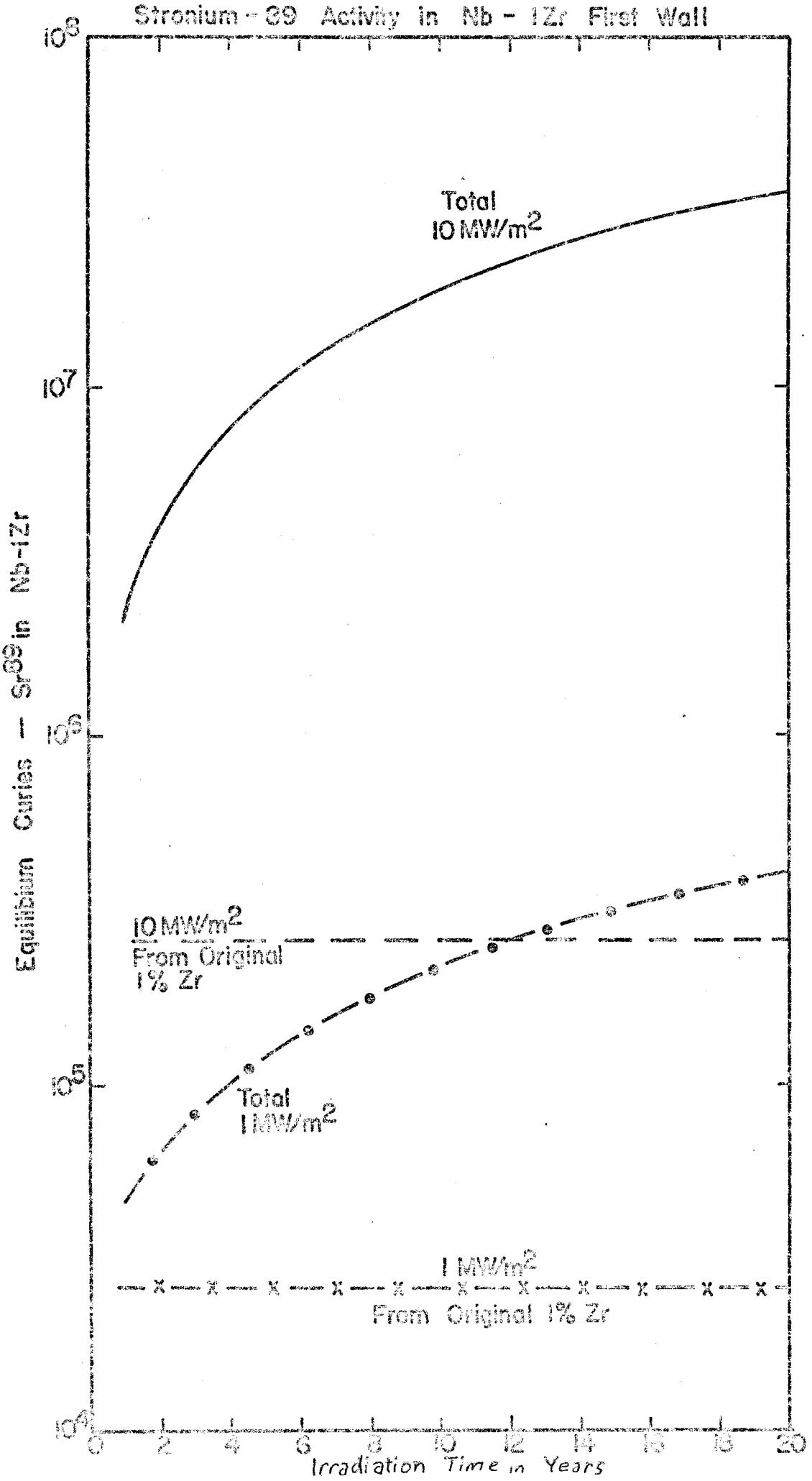
Stronium - 89 Activity in Nb - 1Zr First Wall
Equilibrium Curies - Sr^{89} in Nb-1Zr
10^8
10^7
10^6
10^5
10^4
Total
10 MW/m²
10 MW/m²
From Original
1% Zr
Total
1 MW/m²
1 MW/m²
From Original 1% Zr
0
2
4
6
8
10
12
14
16
18
20
Irradiation Time in Years

Figure IX

APPENDIX B

Results of Calculations

Table 8-1

Summary of Transmutations in V-20Ti

Element	Original Concentration-appm	appm/Mw/m^2/yr New	Burned Up	Net Change
V	~795,000	114.9	276.9	-162
Ti	~200,000	233	180	+ 53
Al	415	0.1	0.4	-0.3
B	5	0.3	0.1	+0.2
Cr	20	99.1	N	+99.1
Fe	100	N	0.2	-0.2
Mn	20	0.2	N	+0.2
Si	640	0.8	1.3	-0.5
C	640	1.8	1	+0.8
N	550	N	0.7	-0.7
O	2550	0.4	1.7	-1.3
Be	N	0.4	N	+0.4
Ca	N	0.9	N	+0.9
Mg	N	0.6	N	+0.6
Na	N	0.2	N	+0.2
Sc	N	9.1	N	+9.1

N = Not reported or negligible

Table A-2

Summary of Gas Production Rates in V-20Ti (First Wall)

From	Original Concentration Of Parent Alloy-appm	appm/MW/m^2/yr He	appm/MW/m^2/yr H	Atomic % He	Atomic % H
V	795,000	62.9	114.9	87.6	52.4
Ti	200,000	4.4	102.8	6.1	46.9
O	2,550	1.3	0.4	1.8	0.2
C	640	2.1	N	2.9	N
N	550	0.3	0.4	0.4	0.2
Si	640	0.5	0.7	0.7	0.3
Al	415	0.3	0.1	0.4	N
	Total	71.8	219.3		

N = negligible, <0.1 amy.

Table 8-3

Summary of Transmutations in Nb-1Zr

Element	Original Concentration appm	appm/MW/m^2/year New	Burned Up	Net Change	
Nb	987,000	2706	4191	-1485	
Zr	10,000	1486	13.1	+1473	(a)
B	9	0.1	N	+0.1	
Si	165	0.2	0.3	-0.1	
Ti	200	0.2	0.2	---	
C	310	0.4	0.5	-0.1	
N	230	N	0.3	-0.3	
O	580	0.1	0.4	-0.3	
Mg	N	0.1	----	+0.1	
Y	N	11.7	----	+11.7	

N = Negligible

a) Zr^{92}, no burn out included

Table B-4

Summary of Gas Production in

Nb-1Zr First Wall Material

From	Original Concentration appm	appm/MW/m^2/year		Atomic Percent	
		He	H	He	H
Nb	987,000	34.6	112	95.9	98.4
Zr	10,000	0.1	1.3	0.3	1.1
N	230	0.1	0.2	0.3	0.2
O	580	0.3	0.1	0.8	0.1
C	310	1.0	N	2.8	N
Si	165	0.1	0.2	0.3	0.2
		36.2	113.8		

N = Negligible

Table B-5

Summary of Major Metallic Transmutation Rates in 316 Stainless Steel

Element	Original Concentration appm	appm/MW/m^2/year New	Burned Up	Net Change
Fe	626,000	253	1,477	-1,224
Cr	180,000	296	272	+ 24
Ni	140,000	44	221	- 177
Mn	20,000	1,213	53	+1,160
Si	14,950	18	30	- 12
Cu	1,000	0.4	6	- 5.6
Al	1,030	0.3	0.9	- 0.6
B	52	0.2	0.3	- 0.1
Co	500	0.3	N	+ 0.3
Nb	300	0.8	1.3	- 0.5
P	360	0.2	0.3	- 0.1
Ti	115	45.1	N	+ 45.1
V	2,200	177.5	0.8	+ 176.7
C	2,800	0.7	4.1	- 3.4
O	400	0.1	0.5	- 0.4
N	400	-	0.5	- 0.5
Be	N	1.6	N	+ 1.6
Mg	N	12.3	N	+ 12.3
Na	N	0.5	N	+ 0.5
Zr	N	0.5	N	+ 0.5

N = Negligible

Table A-6

Summary of Gas Production in 316 Stainless Steel

From	Original Concentration appm	appm/MW/m^2/year		Atomic %	
		He	H	He	H
Fe	626,000	201	310	72.1	48.7
Cr	180,000	44.8	81.9	16.1	12.9
Ni	140,000	6.5	214	2.3	33.6
Mn	20,000	2.6	8	0.9	1.3
Si	14,950	12.6	17.6	4.5	2.8
N	400	0.2	0.3	0.1	N
O	400	0.4	0.1	0.1	N
C	2,800	9.3	N	3.3	N
B	52	0.3	N	0.1	N
Al	1,030	0.5	0.3	0.2	N
V	2,200	0.2	0.3	0.1	N
Cu	1,000	0.1	3.8	N	0.6
P	360	0.2	0.2	0.1	N
		278.7	636.5		

N = Negligible